Granular I/O: Enabling Bi-directional Malleable Interaction for Actuated TUIs with Magnetic Particles

Chi Wang
University of Chicago
Chicago, Illinois, USA
chiwang@uchicago.edu

Clara Cui
University of Chicago
Chicago, Illinois, USA
University of Illinois
Urbana, Illinois, USA
cbcui@uchicago.edu

Alan Pham
University of Chicago
Chicago, Illinois, USA
apham799@uchicago.edu

Justice T Andersen
University of Chicago
Chicago, Illinois, USA
jtandersen@uchicago.edu

Tucker Rae-Grant
Computer Science
University of Chicago
Chicago, Illinois, USA
raegrant@uchicago.edu

Ken Nakagaki
University of Chicago
Chicago, Illinois, USA
knakagaki@uchicago.edu

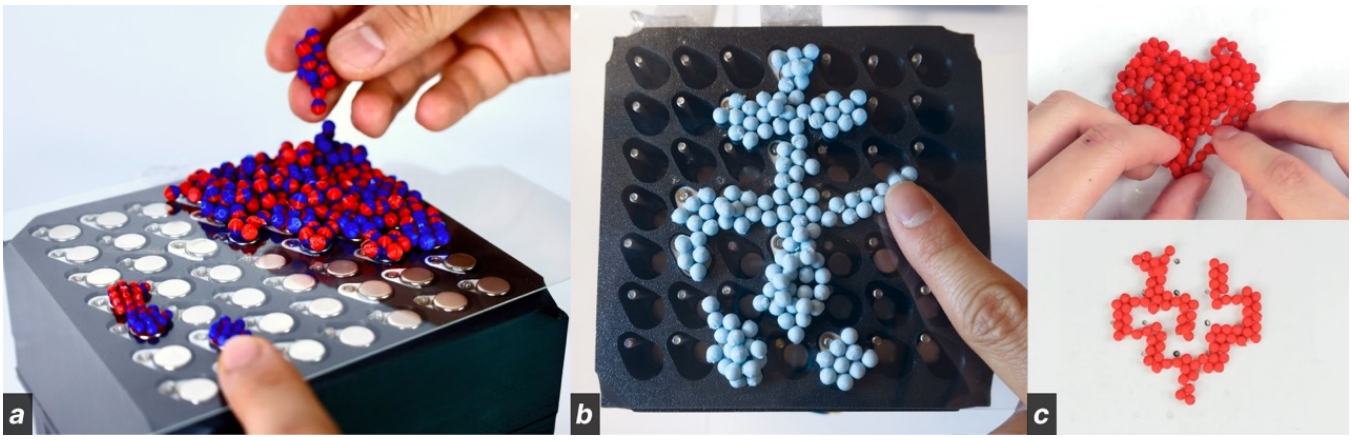


Figure 1: Granular I/O: (a) Magnetic particles on one of the actuation platforms, (b) User interacting with a stick figure consists of particles, (c) User arrange the particles into a heart shape (top) and system record and recreated heart (bottom).

Abstract

Granular materials — clusters of small discrete particles — afford a uniquely malleable form of physical interaction, enabling intuitive shaping, splitting, and merging through natural hand gestures. Despite their rich interaction potential, granular materials remain largely unexplored as a form factor for actuated, bi-directional Tangible User Interfaces (TUIs). We present Granular I/O, an approach that employs millimeter-scale passive magnetic particle clusters, actuated by external magnetic field controllers, to enable malleable input and output interactions for granular-based actuated TUIs. We describe a comprehensive design space for malleable granular interaction, alongside a full hardware and software implementation covering particle cluster fabrication, two actuation platforms, and authoring software. We further report technical characterization and evaluation to validate the system, and demonstrate a range of applications that harness malleable I/O for interactive use.

CCS Concepts

• **Human-centered computing** → **Interaction devices**.

Keywords

Actuated Tangible User Interface; Magnetic Actuation

ACM Reference Format:
Chi Wang, Clara Cui, Alan Pham, Justice T Andersen, Tucker Rae-Grant, and Ken Nakagaki. 2026. Granular I/O: Enabling Bi-directional Malleable Interaction for Actuated TUIs with Magnetic Particles. In *The 39th Annual ACM Symposium on User Interface Software and Technology (UIST '26), November 02–05, 2026, Detroit, MI, USA.* ACM, New York, NY, USA, 15 pages. https://doi.org/10.1145/3830398.3830589

This work is licensed under a Creative Commons Attribution 4.0 International License.
UIST '26, Detroit, MI, USA
© 2026 Copyright held by the owner/author(s).
ACM ISBN 979-8-4007-2856-3/26/11
https://doi.org/10.1145/3830398.3830589

1 Introduction

Granular materials — clusters of small discrete particles — possess a rich set of physical affordances that are unique among everyday substances. Their collective mass is inherently *malleable*: it can

be freely shaped by hand, divided into portions, and merged back together, all through natural, intuitive gestures requiring no tools or special skill. These qualities are deeply familiar from everyday experience: a child sculpts and carves a sandcastle with bare hands; a person sweeps beads into a new arrangement or carefully positions individual pieces; a gardener shapes loose soil into a mound, splits a portion away, or merges two piles together. Across these varied contexts, granular materials invite hands-on engagement — affording *shaping*, *splitting*, and *merging* — that is qualitatively different from how we interact with rigid, sheet, or liquid materials. These properties make granular materials a compelling medium for interaction design, yet they have been underexplored because of the challenge in actuating them.

Within HCI, actuated Tangible User Interfaces (TUIs) [49] and Shape-Changing Interfaces [39] have explored diverse forms inspired by real-world materials and objects to investigate novel I/O modalities with rich affordances [38, 59]. These have included sheet materials[11, 43], threads and fibers[14, 28], playing cards[41], fluids[3, 29, 54, 55], and others. By enabling the actuation of familiar form factors, each of these bodies of work expands on novel interactions and functionalities grounded in how we engage with the material world in daily life. Yet granular materials — with their uniquely malleable and particulate character — have remained largely unaddressed as a form factor for actuated, bi-directional interaction.

Within HCI, granular materials have primarily been explored for input, harnessing their tactile and spatial affordances. SandScape[13], for instance, allowed users to tangibly manipulate the terrain in a sandbox, which was simultaneously captured as digital data to allow for seamless interaction between the physical and digital realms. Some research has employed granular materials for actuation, such as Fluidized Bed Interface[24], Jamming UI[6], and Three-Dimensional Mid-Air Acoustic Manipulation [32, 33]. However, no prior work has comprehensively explored granular material as a form factor supporting both malleable *input* and *output* within a unified actuated TUI. This gap motivates our work: to explore, as an initial step, the interaction affordances of granular materials for bi-directional, actuated systems.

In this paper, we use the term *malleable interaction* — or *malleable I/O* — to describe the unique interactivity and affordances (inspired by [5] [1])of a robotic, actuated system enabled by clusters of granular particles. While malleability as a mechanical property refers to "an ability for something, generally metals, to be molded or deformed into another shape" [2], *malleable interaction* focuses on the interaction itself: the capacity of a dynamic physical interface to be manipulated and shaped both by the user and by the system.

To this end, we propose Granular I/O, an approach for employing granular material — specifically, a cluster of self-attractive particles — as a generalizable form factor for an actuated TUI that affords bi-directional malleable input and output. Granular I/O is designed around three core criteria: **1. Granular Particle Design:** We design a granular particle that supports intuitive hand-shaping of clusters by encapsulating magnets within each particle to allow the group to maintain a given form through cohesive attraction, **2. Actuation of Granular Material:** We develop an actuation method that enables active *malleable* shape change as well as haptic feedback, and **3. Sensing Malleable User Input:** A sensing system captures the user-manipulated state of the granular matter, enabling a complete interaction pipeline between user and system.

To achieve these goals, Granular I/O employs a cluster of magnetically attracted particles at the millimeter-scale (3–5 mm diameter), actuated by an array of computationally controlled magnets and sensed via a computer vision system. A key finding from our prototyping process was that effective malleable actuation requires carefully tuned inter-particle magnetic attraction, rendering bare, commercially available neodymium magnets unsuitable. We thus developed a generalizable method to attenuate attraction force by encapsulating magnets using FDM 3D printing.

In this paper, we present a comprehensive design space for malleable granular input and output interaction. Our proof-of-concept implementation explores two actuation methods — electromagnets [EM] and linearly actuated permanent magnets [LAPM] — for surface-based (2D) shape manipulation of particle clusters. We further developed a 2D computer vision input system to detect user-manipulated shapes and support real-time interactivity, and a set of *actuation primitives* that enable versatile shape manipulation across generic actuation platforms, evaluated through technical characterizations. Together, these contributions are demonstrated through a range of applications that harness malleable I/O to both display information and facilitate expressive user input.

We consider this work an opening of a novel and generalizable form factor for actuated, shape-changing interfaces capable of rich malleable interactivity, in the spirit of seminal visions such as Radical Atoms and Programmable Matter [9, 12, 26].

The list of our contributions includes:

- The concept of *malleable interaction* to describe a class of bidirectional TUIs based on granular materials.
- An approach of using millimeter-scale passive magnetic particle clusters with external magnetic field controllers for *malleable interaction*.
- The implementation of an integrated hardware and software platform for actuating a granular interface, as well as authoring software for designing interactions.
- A technical characterization of our system.
- A demonstration of potential applications for interactivity and a discussion of future opportunities.

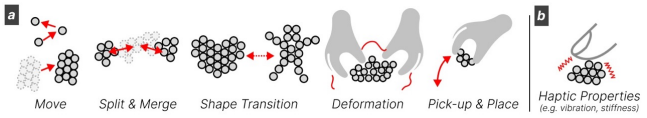


Figure 2: (a) Examples of bi-directional malleable interaction and (b) Haptic property rendering

1.1 Malleable Interaction with Granular I/O

Figure 2a provides examples of bidirectional, malleable interaction performed by the user and the system for Granular I/O. Granular material affords users the ability to *move* individual particles or entire groups ("clusters"). Various redistributive operations can be

[1] [5] referred to the term 'malleable' as an interaction opportunity for inputs, but didn't explore the actuation outputs.
[2] https://www.physicsbook.gatech.edu/Malleability

performed, such as *split and merge* and *shape transition* (or *deformation*). Users can *pick up and place* as an operation for additive and subtractive interaction. Overall, malleable interaction refers to the capability of the granular material to be manipulated bidirectionally through granular and manipulative means. These examples are not meant to be a comprehensive list, but rather provide prominent instances of interaction with granular material that can be afforded. Additionally, Figure 2b shows the added capability of our system to enable *haptic property rendering*, such as *vibration* and *stiffness-change* beyond geometrical manipulation.

As a first bidirectional granular material actuation system, Granular I/O is designed with the range of malleable interactivity in mind. As a foundational step, our implementation focuses on 2D surface-based granular material interaction; 3D shape construction and input remain open challenges, even though the material itself physically affords 3D manipulation.

2 Related Work

Granular I/O is built on diverse literature, including programmable matter, modular and swarm robotics and UIs, interfaces employing granular materials, and magnetic actuation systems.

2.1 Programmable Matter and Modular Robotics

Programmable Matter [26], coined by Toffoli and Margolus in 1991, was defined as "an ensemble of fine-grained computing elements arranged in space[53]." Inspired by this concept, in the early 2000s, Goldstein, Mowry et al. developed Claytronics [9], implementing modular components consisting of computing and actuation elements that each particle could dynamically reconfigure, envisioning a future where these could be miniaturized to the nano-scale.

This line of research heavily influenced work in Modular Robotics [48, 65], which produced modular robotic components that can reconfigure to take diverse geometric and kinematic forms to serve different tasks, including m-Blocks [42] (5 cm-cube, flywheel-embedded self-reconfigurable systems) and Robotic Pebble [8] (1 cm-cube, supporting passive assembly without dynamic self-reconfiguration). In HCI, the engineering and deployment of modular robotic components have also been actively explored. For example, the Swarm User Interface [17], which proposed self-locomoting tabletop multi-robot systems for display and interaction, was partly influenced by Swarm Robotics research [2, 44]. The concept and implementation of Swarm UIs have inspired a cluster of actuated modules with rich input and output manipulability, harnessing the affordance of cluster sizes between "objects" and "particles".

Although the original Programmable Matter vision of "fine-grained elements" influenced seminal research, scaling down individual robotic elements (containing computers, actuators, batteries, etc.) has remained a technical challenge. While exciting results have been demonstrated in both HCI and robotics, pursuing this vision via self-contained robotic devices presents a bottleneck for scaling toward "fine-grained elements" capable of reconfiguring themselves. To this end, we approach the scope of the programmable matter concept by exploring the actuation of passive particles and granular materials using external actuation energy, namely a magnetic field, while focusing on the malleable interaction.

2.2 Interactive Granular, Passive Materials

While diverse malleable materials, including fluids, have been explored as actuated interfaces [46, 56], the idea of employing passive granular particles or modules has been explored in HCI. For example, passive granular particles were used to provide rich affordances for users manipulating 3D terrain, as in SandScape [13]. The Jamming User Interface [6] and ClaytricSurface [23] explored granular material in vacuum-sealed deformable membranes as stiffness-changing malleable materials. As such, TUIs based on granular particles offer significant advantages in providing rich malleable affordances.

Within HCI, actuating passive materials or modules has been explored under the concepts of Shape-Changing Interfaces and Shape Displays [7, 40]. Kinetic Blocks [47] demonstrated the manipulation of passive magnet-embedded blocks (5 cm cubes) assembled via a pin-based shape display. DynaBlock [52] advanced this approach by shrinking individual modules to 9 mm cubic units, using a magnet-based interlocking design controlled by a linear-actuator array to create 3D geometries.

Towards reconfiguring finer granular materials, prior work has employed non-contact ultrasonic acoustic actuation to manipulate light particles on a 2D surface [22], to levitate clusters of granular particles in mid-air [32, 33], to rotate individual beads of a mid-air display [45], and to assemble particles or small modules one by one [4]. While acoustic actuation enables precise manipulation of fine objects (e.g. as acoustic tweezers), malleable I/O of granular particles — where users can deform, shape, and manipulate materials bidirectionally — remains largely unexplored.

Several studies have explored actuating granular materials to enable global, dynamic stiffness or property changes, including Jamming [6, 23] and the Fluidized Bed Interface [24], affecting the malleability or haptics of the interface. However, leveraging actuated granular materials to enhance both malleable input and output — and to harness their rich affordances — remains underexplored.

2.3 Magnetic Actuation and Microrobots

Magnet-based actuation for tangible, actuated UIs has been actively explored in HCI, including levitating tangible UI [18] and shape-changing deformable materials [50].

One of the standard actuation methods for tabletop tangible actuation has been to develop computationally controlled magnet arrays. An early example of this was the Actuated Workbench[35], which explored control methods for using an electromagnet (EM) array to actuate the magnet pucks on top of it. Madget [58] used a similar EM array as an actuation device, but extended the actuatable components to widgets like sliders and knobs. Reactile [51] employed an array of PCB coils to actuate the 2D position of 10 mm magnet-embedded tangibles for interaction. Our work similarly uses a grid array of magnetic actuators (e.g. EM or linearly actuated permanent magnets) but explores magnetic particle actuation. While some prior research explored magnetically actuating fluids [15, 57]and clay materials [61], our approach of actuating granular particles focuses on the interaction space between centimeter-scale blocks and fluid-like elements.

On the other hand, robotics researchers have studied particles' behavior at the millimeter scale with magnetic *microrobots* research.

Microrobots are robotic systems that integrate sensing, actuation, and/or control, often powered or guided by external fields at the micrometer-to-millimeter scale. They are designed for tasks like biomedical intervention, micromanipulation, or collective robotic research. Recent works, for example, presented magnetic microbots at a scale of 0.3 x 0.3 x 0.6mm [19, 62] and 1.8mm cube [1], as well as diamagnetically levitated robots at 2 x 2 x 0.5 mm [36]. While extensive motion control methods have been proposed and evaluated for microrobots ~1 mm in size, the unique possibilities for display and tangible interaction at this scale have not been explored. Thus, we also contribute to HCI, specifically in the actuated, interactive material realm, techniques for manipulating millimeter-scale magnetic particles (3-5mm) with computationally controlled magnetic arrays (one of the standards for actuated tabletop TUI in HCI [35, 51, 58]), presenting generalizable control methods for magnetic particles, defined as *actuation primitives*.

Lastly, one of our supplemental contributions includes fine-tuned magnetic attraction for passive particles, which was partially inspired by prior research exploring the magnetic strength and geometry of modules [37] for the vision of Molecular HCI [37], while our approach considers magnetic strength as it supports bidirectional malleable I/O.

3 Implementation and Methods

With Granular I/O, we explore the approach to manipulate passive granular, magnetic materials for bidirectional malleable interaction, where both the system and the users can dynamically manipulate the granular materials.

To explore this approach, we implemented proof-of-concept prototypes consisting of two types of magnetic actuator arrays, custom magnetic particles with tuned attraction force produced via an accessible fabrication method, and control software, which includes the GUI and control algorithms that perform the actuation methods with arrays of magnetic controllers. The overall physical interface is shown in Figure 3. Each implementation detail and generalizable technical method is described below. All the code, design files, and PCB files are available on GitHub.[3]

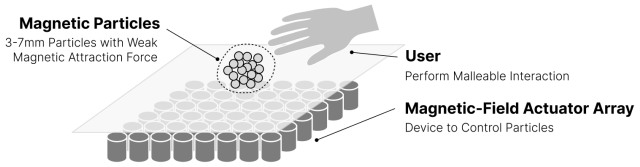


Figure 3: Physical interaction with Granular I/O involves the user, magnetic particles joined into granular clusters, and a magnetic field actuator array.

3.1 Magnetic Particles: Design and Fabrication

When designing the particles for Granular I/O, our goal was to support both direct manipulation by the user and control by the system, enabling bidirectional malleable interaction. We proposed to use millimeter-scale magnetic particles as the malleable medium for an actuated TUI. While prototyping, we found that one of the most important design considerations for the magnetic particles was to have a relatively weak strength of self-attraction relative to the strength of the magnetic control system. Prior research has introduced different candidate methods for fabricating such weak magnetic particles. One such method is to use custom magnetic compounds with tunable properties [25, 34, 62], yet these methods require chemical processes, such as material molding and casting. Another method is to incorporate reprogrammable magnetic sheets [30, 31, 63, 64], but we require the particles to be actuated by a strong, dynamic magnetic field, and such reprogrammable materials would be prone to demagnetization under repeated exposure, making them less suitable. For our research, we developed a more accessible method to fabricate 'weak' attraction magnetic particles using magnets enclosed in 3D-printed shells.

Specifically, we used a Bambu Lab A1 Printer with a 0.2 mm nozzle and PLA filament for the enclosures. Figure 4 shows the printing processes. For the magnets, we settled on two options based on the target particle size. For particles in the 4-7 mm range, we use commonly available, 3 mm diameter toy magnetic beads[4]. For smaller particles, we use 1.5 mm cube N42-grade magnets, which are also commercially available[5].

We provide a performance evaluation of different configurations of magnet and shell in the appendix (section C), but our rough target for weakening the self-attraction of the magnets was to reduce their magnetic strength by one order of magnitude (e.g. from 300 mT to ~30 mT). We found that shell thicknesses of 1 mm for the 3 mm spherical magnets and 0.5 mm for the 1.5 mm cubic magnets achieved reductions in this range. Additionally, using a 3D printer to fabricate the shells allowed us to customize other aspects of the particles, such as their color, shape, and material. For example, we employed a two-tone, red and blue color scheme, which helped us visualize the polarity of particles when applying magnetic fields. Meanwhile, we also experimented with different shapes and observed that cubes tend to align more in grid/linear configurations, while spheres form rather organic configurations, as seen in Figure 3.1a. We also present an example that uses PVA filament to allow users to fuse clusters together by spraying them with water.

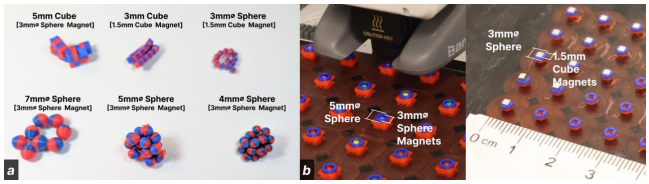


Figure 4: (a) Six kinds of particles we evaluated. (b) Inserting magnets in the middle of 3D printing.

3.2 Control Hardware

We explored two approaches to engineering magnetic field actuator arrays: one utilizing electromagnets (EM Array) and the other using

[3]https://github.com/AxLab-UofC/GranularIO

[4]https://www.amazon.com/1000PCS-Magnetic-Building-Anti-Anxiety-Relaxation/dp/B0GRPQJFJZ/

[5]https://www.kjmagnetics.com/b111-neodymium-block-magnet

permanent magnets mounted on linear actuators (LAPM Array). The design of the actuator array should carefully balance the *control resolution*, *magnetic strength*, and *response time*. Our proposed approaches and their key characteristics are shown in Figure 5. This section first introduces how we implemented these two systems, and then provides design considerations for control arrays based on their differences.

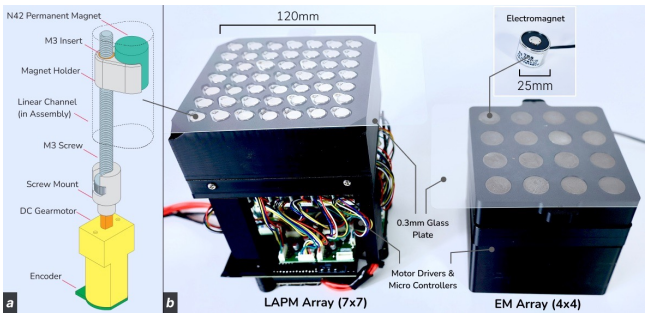


Figure 5: (a) Exploded view of LAPM (Linear Actuated Permanent Magnet), (b) Two magnetic field actuator arrays (From Left-to-Right): LAPM and EM (Electromagnet) Arrays

3.2.1 Electromagnet(EM) Array. The electromagnet array consists of 16 off-the-shelf electromagnets (12V DC, 25 mm diameter, 20 mm height) arranged in a 4 x 4 grid with 26 mm spacing center-to-center, which are encased in a 3D-printed PLA enclosure. Through prototyping, we found that adding an 18 mm diameter by 3 mm thick steel disk on top of each electromagnet increased the magnetic field area. The maximum measured magnetic strength at the interaction surface was 70 mT, and the response time to change the intensity is less than 0.01 s. When actuating particles, the maximum vibration frequency is ~500 Hz (limited by our implemented firmware on the micro controller), and the time to flip over an individual particle is ~0.3 s. The electromagnets are driven by 4 Adafruit Feather Wing DC motor drivers, which are controlled by one Teensy 3.2 via I2C (see Figure 6).

3.2.2 Linear Actuated Permanent Magnets(LAPM) Array. Our second hardware implementation takes advantage of the strong magnetic fields of N42 grade NdFeB magnets, but this strength introduces a new design problem: large pull forces are required to raise and lower these magnets in order to change the magnetic field strength at the interaction surface. To achieve a strong pull force while also optimizing for speed, we carefully selected the motor, gearbox ratio, and lead screw pitch for the linear actuators. In each actuation unit, as shown in Figure 5a, the 3/8 x 1/2 inch permanent magnet is connected to a linear rail with a 3D-printed holder containing an M3 heat insert. The linear rail is an M3 x 40 mm screw with a stroke of 24 mm and is actuated by an N20 DC Motor with a gearbox ratio of 10:1, rated at 1000 rpm and 15mN · m stall torque. The combined magnet and linear actuator units are spaced 15 mm center-to-center, and our prototype consists of a 7 x 7 actuator array. The maximum measured magnetic strength at the interaction surface was 566 mT, and our actuators take an average of 1.7s to fully lower from their highest position, providing an average magnetic field rate of change of 332.9 mT/s.

Group	Characteristic	EM Array	LAPM Array
Strength Density	*Pitch / Distance Center-to-center*	26 mm	**15 mm**
	Max. Magnetic Strength	70 mT	**566 mT**
Dynamics	*Response Time*	**<0.01 s**	<1.7 s
	Polarity Reversal	**Yes**	No
Fabrication	*$ / Actuator*	~$20 USD	~$20 USD
	Assembly	**Simple**	Complex
	Min. Height	**20 mm**	150 mm

Table 1: Comparison of the EM and LAPM Arrays.

The drive electronics for the LAPM array are shown in Figure 6 and includes a motherboard, 4 Teensy 3.2s, and 14 motor driver boards. The motherboard distributes the power for the motor drivers and connects I2C communication and encoder signals between the Teensy 3.2s and the motor drivers. The custom motor driver shares the same schematic as the Adafruit Feather Wing DC motor drivers used in the EM array, with a PCA9685 chip for I2C communication with the Teensy and two TB6612FNG chips to drive up to 4 motors. We designed the layout of the PCB to be compact and to bypass the encoder signals from the motors to the motherboard, further simplifying the wiring required during assembly.

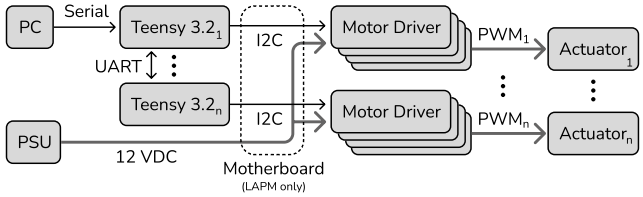


Figure 6: Control Hardware Electronic Architecture.

3.2.3 Control Hardware Comparison. While the two styles of control hardware share a similar electronic structure as well as layout, each of them has distinct characteristics due to the difference in magnetic field generation. Through testing and prototyping, we found each to have its own advantages and disadvantages for serving the goal of Granular I/O to manipulate passive magnetic clusters. With the two different hardware styles, we intend to explore the wide possibilities of the Granular I/O concept, where EM and LAPM complement each other to explore broader actuation opportunities for interaction. Therefore, there are pros and cons for each hardware; they differ in suitable actuation functionality. Table 1 shows a general comparison between the EM and LAPM arrays, including both qualitative distinctions and lab measurements, which are shown in brackets. This is meant to provide generalizable guidance to help future researchers select from different control hardware options based on their goals. We divide the comparative characteristics into three major groups.

The first key group of parameters is **Strength Density**, which compares the performance of the center-to-center pitch of the actuators and their peak magnetic strength. Generally, neodymium magnets have a stronger magnetic field and a higher actuator density

compared to the electromagnets. With our prototype, a neodymium magnet (9.5 x 12.7 mm cylinder, 3/8 x 1/2 inch) measured a maximum magnetic strength of 566 mT while a larger electromagnet (25 mm x 20 mm) measured a much smaller peak strength (70mT). Peak magnetic strength directly affects how firmly the system can manipulate particles, and a stronger magnetic field also allows for a wider range of stiffness representations. Additionally, the actuator pitch directly correlates to the resolution of the magnetic field array – important when a high-resolution display is desired.

The second key group of comparative parameters is **Dynamics**, meaning the ability of the system to modulate the magnetic field at the interaction surface. Specifically, EMs have a more dynamic controllability than LAPMs because they can rapidly switch the magnetic field on and off. Furthermore, EMs can reverse the polarity for individual actuators, whereas LAPMs are constrained to a singular polarity. Due to these characteristics, the EM Array is preferable when applications require high controllability, for example, when creating fast oscillations (e.g., vibration), or when making individual particles flip over. Those actuations are difficult to perform using a single actuator with the LAPM array.

In addition to these two key groups of characteristics, there are other factors that future researchers and designers could take into account. Specifically, while the price per actuator is similar (both around $20 USD) the EMs require much less assembly compared to the LAPM, which employs a custom linear actuation mechanism. The LAPM also requires more Z-height space within the control hardware, which may not be preferable when needing a lower-profile mechanism.

While different component selections would result in different characteristics, we present these measurements to underline the fact that the control hardware should be selected strategically.

3.3 Actuation Methods

In this section, we describe the methods used to actuate the particles — specifically, the development of control patterns for the actuator array (applicable for both EM and LAPM).

To achieve manipulation of granular material shapes, we developed two primary actuation methods: (1) A primitive, local control method that manipulates a cluster of particles through *bottom-up, individual pixel-oriented control*, which we call *Actuation Primitives*, and (2) *A global, top-down control method* that takes a target arbitrary geometry as input and translates the overall shape accordingly, which we call *Shape Transition*. Within the authoring software tool (described in section 3.4.1), *Actuation Primitives* allow users to locally assign primitive actuations to specific actuator pixels, while *Shape Transition* allows users to specify an overall target shape for the system to configure automatically. The details of each control method are described below.

3.3.1 Actuation Primitives. Actuation Primitives (AP) are local control methods to identify each actuator pixel to perform basic *primitive* actuation, which includes **move**, **split**, and haptic **vibration** and **stiffness change**. These primitives are elicited from our motivation to develop the basic malleable interaction shown in Figure 2, except for the Shape Transition, which we consider as a global control method. In Figure 7, we illustrate how these are implemented with our control hardware, and we detail one by one below.

Move: As shown in Figure 7a, the **default-move** is implemented in a stepwise process similar to prior works [35, 58]. In each step, the system turns the next magnetic pixel in the path on at a high strength and subsequently turns the previous pixel off. This on-off sequence is repeated for the entire path. When moving particles with electromagnets, we add an additional step of turning the previous pixel briefly to the opposite polarity before turning off, as this improves the moving success rate.

Unlike the near-instantaneous response with electromagnets, when moving particles with the permanent magnets, the pixel response time becomes a bottleneck for improving the movement speed. As the target move speed increases, the pixel may not have enough time to fully turn on to attract the particles from the previous pixel. To improve the movement speed for LAPM, we implemented a method to turn on all pixels in the path so that at every step the next pixel will always be attracting at maximum intensity, as illustrated in Figure 7b, **fast-lapm-move**. The cost of this approach is that all the pixels in the path are occupied during this move, and may not be used to complete other actuation. We further evaluate the maximum moving speed in Section 5.1.

Split: Different types of hardware handle splitting differently.

For the LAPM array, as shown in Figure 7c, the general approach for splitting involves actuating 3 pixels in a row, namely the starting, intermediate, and target pixels. Starting from [*c1*], the intermediate and target pixels turn on [c2], then the starting pixel's intensity is reduced by d, and the intermediate pixel by $d/2$ [c3]. Then, all the pixels turn on to maximum strength [c4] and finally complete the split by turning off the intermediate pixel [c5]. A key step here is [c3], where the particles transferred to the target pixel depend on the intensity-difference parameter d. To understand how d would affect the splitting ratio, we evaluated the splitting particle amount with different d in Section 5.

For the EM array, as shown in Figure 7d, the splitting approach also involves 3 pixels, including a starting pixel and 2 neighboring pixels. A key step in splitting is [d2], where the starting pixel will oscillate to split the cluster to its 2 neighboring pixels.

Stiffness: As shown in Figure 7e, both devices support changing the cluster's stiffness by running at different intensities. The stronger the intensity, the stiffer the particles feel.

As a reference, we provide a preliminary comparison between the two devices. We used a force gauge attached to a planar surface to measure the maximum force while gradually compressing a cuboid cluster of ~135 particles, each 5-mm in diameter, until they settled into a single layer of particles. On the EM platform operating at maximum magnetic strength, 4.5 N was measured and 60.4 N was measured for the LAPM platform. As a baseline, 2.1 N was measured without magnetic actuators.

Vibration: As shown in Figure 7f, the unique capability of electromagnets to generate oscillating magnetic fields enables the EM array to create a vibration. The particles' vibration intensity is positively correlated with the oscillation intensity, and the vibration frequency is the same as oscillation frequency.

3.3.2 Shape Transition. For the top-down *Shape Transition* method, we defined the challenges for enabling the control as follows: from any starting shape, the system should render the target shape automatically. In this paper, we developed the shape transition actuation

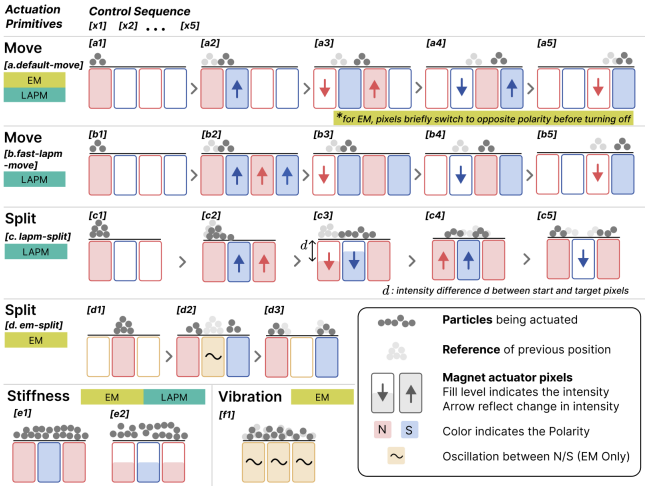


Figure 7: Implementation of Actuation Primitives. The Control Sequences illustrate actuator patterns for various APs with specific Control Hardware (EM/LAPM)

only with the LAPM array because of the larger actuator counts (7x7), compared to the EM array (4 x 4).

A naive approach to performing shape transition would be to simultaneously turn on all of the magnets in the target shape region, but we found that this does not work due to the fact that the magnetic actuators have a limited effect range. As shown in Appendix B, the magnetic field intensity for our actuators decays with distance r at a rate of approximately $1/e^r$, and the magnetic field drops to near background level after reaching the center of the neighboring pixel. This limited effect range creates two problems for shape transition:

(1) The particles will not distribute evenly across the target shape, since more distant target pixels will not be able to attract particles from the original shape.
(2) For shapes that are not adjacent, target pixels might not be able to attract any particles from their starting positions.

To tackle the problem of uneven distribution, we propose a control method called "shaking". As shown in Figure 8, by alternatively activating and deactivating the magnet, we can redistribute the particles across the platform. However, this method is not effective for particles in regions larger than the adjacent 8 pixels.

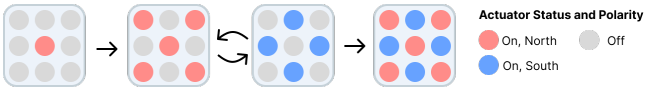


Figure 8: Illustration of the "shaking" process, by alternating turning on/off the adjacent magnets

To address the second problem where particles are not passed between shapes that are not adjacent, we were inspired by an animation technique called "tweening"[16, 60] that generates intermediate frames to create a smooth motion. We developed a custom-built algorithm that creates a set of tweening frames to help connect the gap between the distant shapes. The algorithm is applicable to arbitrary starting and ending shapes and typically completes the transition between two 7x7 pixel frames in about 3 intermediate steps, rarely requiring more than 8 steps. The detailed frame generation algorithm and example tweening frames are shared in Appendix A.

By combining these two methods together, we get our current shape transition pipeline which is as follows: Given a starting shape and a target shape, we generate the tweening frames, where the connecting frames are close to each other. We then use the shaking process to complete the transition between frames. We discuss the quality of the algorithm in Section 5.3.

3.4 Software Architecture and Workflow

Overall, the software for our system consists of a GUI authoring tool written in Processing on the computer and firmware written in C++ (Arduino) on the control hardware. The authoring tool allows users to select actuation methods and execute them on the control array. This software and architecture are applicable to both types of actuator array; the program selects the control methods corresponding to the specified hardware type.

In this section, we will mainly discuss the authoring tool, the associated GUI, and the sensing algorithm.

3.4.1 Authoring Tool & GUI. The authoring tool implements a pipeline to convert user inputs on the GUI into commands for each individual magnet actuator or to trigger sensing from the camera.

As shown in Figure 9, our GUI features a mode selector that allows the user to select between various control modes, including basic actuation primitives (move, split, merge, etc), as well as functions that support the shape transition. Additionally, it displays a live camera feed overlapping a visualization of the strength and polarity of each pixel in the magnetic field actuator array. The workflow is as follows:

For the **Actuation Primitives**, users choose the control mode in the selector mode panel, and choose the location and related parameters to customize their behavior. The raw motor command is generated based on the control sequence illustrated in Figure 7.

To support using the **Shape Transition** functions, we designed a process for inputting shapes and generating a preview for tweening frames and execution. First, to input a target shape, the user can draw with a mouse on the grid or create the desired shape by hand and use the built-in sensing system (discussed below) to detect the shape. Once the user has the desired target shape sequence, the system automatically checks if the target shapes are far from each other and generates tweening frames if necessary for the user to review. The user then executes the frames after reviewing them. The raw motor commands are generated based on the shaping process illustrated in Figure 8.

3.4.2 Sensing. The sensing system captures user-manipulated granular shapes and encodes them as binary occupancy data for use in the authoring tool — for example, to record hand-authored animation frames.

When a frame is captured via the GUI, a top-down image from a USB camera (Logitech BRIO, mounted 20 cm above the interaction surface) is processed into a 7 x 7 binary occupancy grid aligned to

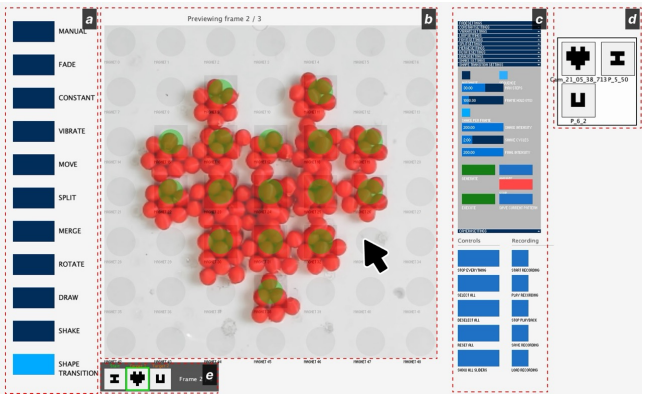


Figure 9: The GUI Interface consists of (a) Control mode selector panel, (b) Actuator control grid with a camera overlay, (c) Parameter configuration and control execution, (d) Saved shape repository, (e) Tweening frames preview.

the LAPM actuator array. The pipeline applies grayscale conversion followed by spatial binning: the image is divided into a 7 x 7 grid of equal regions, and pixel occupancy is computed for each cell by counting pixels below a brightness threshold. Since the background is white, any brightness deviation reliably indicates particle presence, independent of particle color. Each cell is then classified as occupied or empty by comparing its dark-pixel ratio to a tunable threshold, producing the final binary grid.

In our configuration — a well-lit environment with 5 mm particles and 15 x 15 mm grid cells — a threshold of approximately 30% dark pixels per cell yielded reliable shape detection. Both the brightness threshold and the per-cell pixel count threshold are adjustable in the software to accommodate varying particle sizes and lighting conditions. Figure9D shows example detections.

4 Application Space

This section provides a demonstration of potential application spaces using our prototype. In each application, we highlight how the malleable interaction (defined in Figure 2) of Granular I/O is utilized in *italic*.

4.1 Dynamic Shape Display with Haptic Effects

Firstly, with the capability of using particle material to render geometries dynamically, we can render dynamic shapes for display and interaction. Figure 10a represents how Granular I/O utilizes *shape transition* to express tangible displays, such as a heart geometry with dynamic beating movement, fully-shaped from scratch by feeding particles from a feeder box. This could be used to express an affective message to remote partners or to display medical data in a tangible form that can be felt by touching. Figure 10b shows the geometry rendered as a human stick-figure and uses the stiffness control capability to computationally decide which part of the geometry should be locked or free to control by the users. Here, we present a mock-up interaction; if the particle movements by user inputs could be recorded by an additional tracking system, it can create a record and replay movement for users to add animated character expression. As a display, it can not only render shapes but also exhibit additional layers of *haptic properties* such as stiffness and vibration to represent additional dimensions to the shaped digital model (Figure 10c). Not only cluster representation, but also the individual particle movements could be used to express granular element representation, such as a visualization of electron movements in Figure 10d, which highlights the potential of Granular I/O as a tangible educational tool for museum exhibition or textbook augmentation.

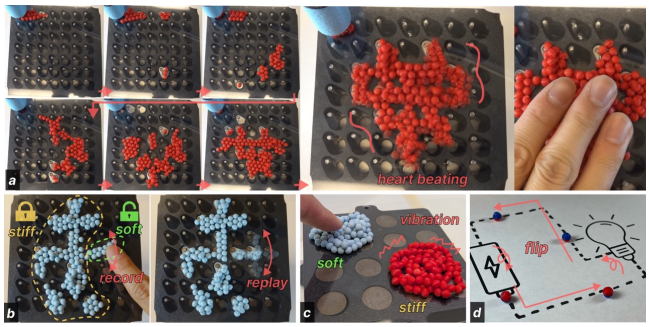


Figure 10: Shape Display with Dynamic Motion and Haptic Properties, including (a) Heart forming and beating, (b) Animating stick-figure, (c) haptic display with different stiffness and vibration, and (d) a particle animation to express electron movement within a circuit.

4.2 Dynamic TUI and Assistance on Tabletop

As Granular I/O takes 2D plane geometry to render shapes, the system could be infused into everyday tabletop surfaces for interactivity. Figure 11 shows how the particles can dynamically render physical UI elements for dynamic physical affordances [7], rendering dynamic buttons and sliders through *move* and *shape transition* (e.g. to control music formed by particles). As a tabletop interface, the system could bring passive tabletop objects to users, such as keys, before they leave the table. While the interactions presented in this demonstration are mock-ups, our camera system can be updated to detect a hand gesture to enable them.

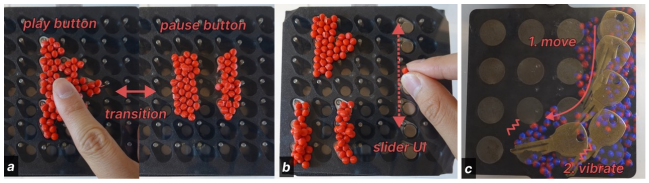


Figure 11: Reconfigurable Tabletop UI for (a) play and pause buttons, (b) interactive volume slider, and (c) Desktop Assistance, moving key to users and alerting with vibration.

4.3 Fabrication and Prototyping

Inspired by DynaBlock [52], we present how dynamic geometries can be rendered with Granular I/O for users to *pick up* dynamically

rendered physical shapes, *deform* for adjustment, and employ for utilities, which we consider a powerful medium for prototyping 3D geometries. As shown in Figure 12, users can "download" a 3D model to be loaded with the particles/clusters. Then, the user can adjust the shape through *deformation* and then *pick* it up. Once they are happy with the shape, they can "lock" the geometry by spraying water onto the PVA particles, which will solidify the design, to be used for a key tag, for example.

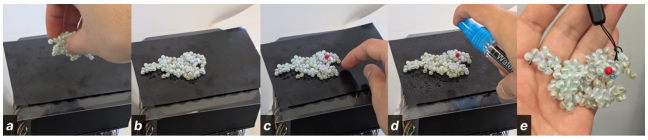


Figure 12: Prototyping using PVA-based particles. (a) a user places a cluster on the platform, (b) the system shapes the cluster based on data selected by the user, (c) the user modifies the shape manually, (d) once they are happy, they apply water and wait for it to solidify, and (e) once solidified, the object can be used as a key chain.) - In this scenario, the user is creating a fish shape, completed by adding a red particle, inspired by the story, 'Swimmy'[21]

4.4 Stop Motion Messages

In this application, the system performs stop-motion playback to display a message composed of sequential shapes created by the user. This mode has the user interact with the particles through *deformation* to form their own "manually-shaped" message, which is then recorded by the system and added to a sequence of messages that can be repeated. For example (as illustrated in Figure 13, if a user wanted to communicate a revealing love message to another user, they could form the following shapes in sequential order ("I", "♡", "U"), saving each frame as a sequence. After the user has completed this message, they can move the particles to obfuscate it. The receiving user can then come to observe the manipulated shapes replicated by the system via *shape transition*.

5 Technical Demonstration

In this section, we will demonstrate the actuation capabilities of Granular I/O, focusing on three main categories: (1) Movement Speed, (2) Splitting Control, and (3) Shape Transition – three key malleable actuation categories as in Figure 2.

5.1 Movement Speed

To evaluate the system's movement speed, we performed trials moving the particle(s) from one corner of the platform to the opposite corner (e.g., from the bottom-left corner to the top-right) and then back to the original corner. Furthermore, as the movement of the particle(s) largely depends on the speed of the magnets and intensity of the neighboring magnetic field, we are mainly concerned with the movement speed that the particle(s) can sustain. In the context of the evaluation, this means that the single particle is able to reach the target, and that the group is able to reach the target

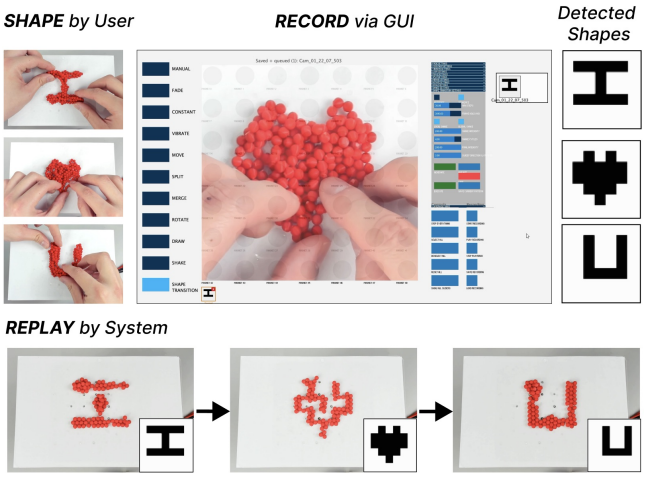


Figure 13: Stop Motion Messages showing the *Shape, Record, Replay* process.

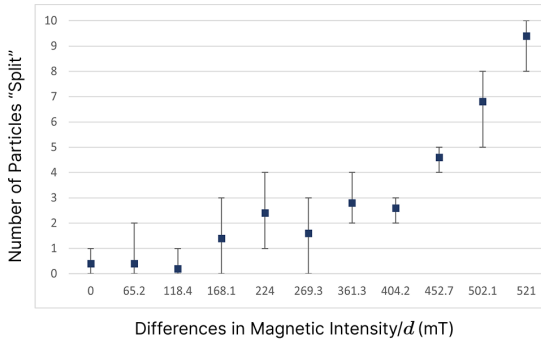


Figure 14: Number of Particles "Split" By Increasing the Magnetic Intensity Difference

without any particles being left behind. Thus, we report the maximum sustainable movement speed utilizing the different actuation platforms and movement methods.

From our evaluation on sustainable movement speed, we found that with LAPM, a group of 10 particles sustained faster movement speed than a single particle. On the LAPM array, with the default-move method (Figure 3.3.1a), the group sustained 23 mm/s versus the single particle's 30 mm/s. Using the fast-lapm-move method (Figure 3.3.1b), the group sustained a movement speed of 46 mm/s whereas a single particle sustained 39 mm/s. Furthermore, we found that EM performance was comparatively better, likely due to the fast response speed of the electromagnets. When using the default-move method with 15 particles, EM sustained 64 mm/s. This improvement by the EM platform compared to the LAPM platform aligns with our characterization of the EM platform from Table 1.

5.2 Split Control

To characterize the granularity of control when performing the split, we conducted the lapm-split (previously introduced in Section 3.3.1) with 10 particles as a preliminary evaluation and recorded

the number of particles that transferred to the target pixel (split). As illustrated in Figure 7c, the splitting control is varied by the intensity differences between the start and target pixels. We performed tests at intervals of ~50mT as shown in Figure 14, repeating 5 times for each interval. As can be seen in Figure 14, the number of particles that successfully split maintains a positive correlation with the difference in magnetic intensity. As a difference of 521mT closely corresponds to the intensity difference in basic particle movement, our findings align with our expectations. While we have demonstrated a capability of controlling the number of particles in a group that split with the LAPM array, future work could be done to have a more fine-grain control of group splitting.

5.3 Shape Transition

As the particles can be reconfigured to transition between shapes, it is beneficial to have an understanding of these capabilities and how they can be affected. As shown in Figure 15, we present the results of transitions from the start frame to the target frame, where the target frame is distinguished by black-outlined circles representing active magnets. This table provides demonstrations of basic geometric transformations (i.e. translation, rotation, compression, and expansion) and actuation methods (i.e. shaking and tweening) introduced in Section 3.3.2.

In Figure 15, we demonstrate the breadth of capabilities of Granular I/O, as well as the benefits of tweening and shaking towards an even distribution of particles over a large range. Because the LAPM array consists of a larger number of pixels which is suitable for shape representation compared to EM array, here, we focus the shape transition demonstration on LAPM. Across the five results overlaid in the leftmost result columns, we observe that the particles tend to fall within the same general area, evenly spread across the intended target area, utilizing the particles' high granularity to create a clear shape. Conversely, the absence of tweening not only decreases the range of distances that a shape is able to transition but also makes the distribution of the particles uneven. As can be seen in the no tweening columns of Figure 15, shapes that are not adjacent to each other can fail to transition entirely or will favor one side of the target shape (potentially due to slight differences in magnetic strength across different magnets, slightly uneven surface, etc.). Similarly, the absence of shaking is demonstrated to decrease the even spread of the particles, as there is no opportunity for the particles to adjust.

While we have demonstrated the capabilities of Granular I/O in shape transition, we observed that the system is limited in transitioning between shapes of different surface areas (as shown in the bottom two rows of Figure 15.

This could be attributed to the fixed volume of the particles which cannot be as easily compressed or expanded compared to other discussed materials such as fluids. While we have observed instances of the particles"hopping" up into the air, it is not consistent enough to be utilized in effectively changing the volume of the shape. Thus, future work could explore improving "hopping" or various methods to improve the compression and expansion of the particles.

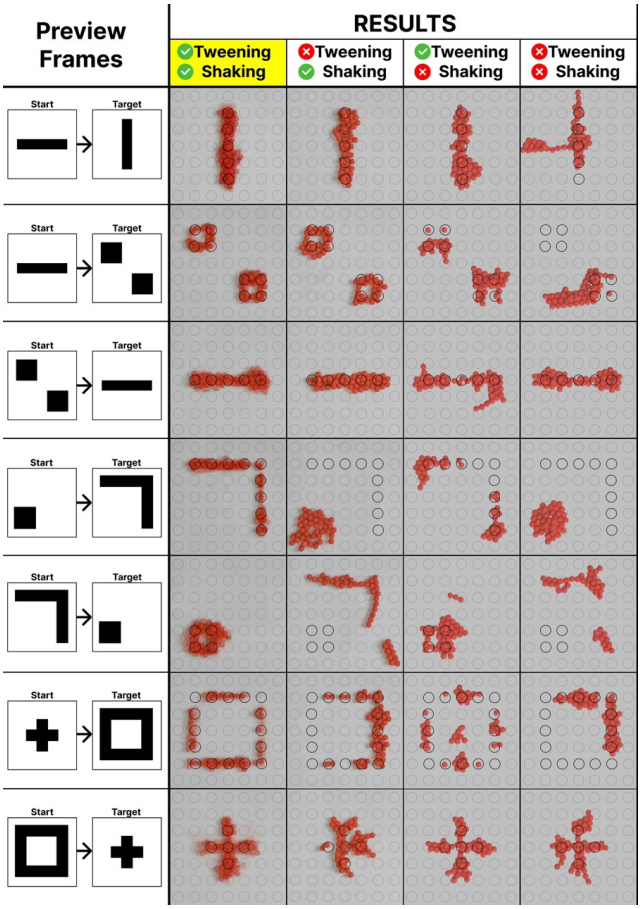


Figure 15: Shape Transition Results (from left-to-right): using tweening and shaking, no tweening but shaking, tweening but no shaking, and no tweening nor shaking.

6 Limitations and Future work

With Granular I/O, we have introduced an approach that enriches the possibilities of physical interaction using actuated magnetic particles. In this section, we discuss the limitations and future work of the system and its general approach.

6.1 Improving the Actuation for Scaling Down and 3D Shapes

We study a limited range of particle sizes and control hardware, and in the future, we would like to further study the relationship between magnet array resolution, magnetic particle size/geometry/material, and magnetic strength to develop comprehensive design guidelines. We believe a computational physics simulation tool could help with the design of particles and support finer control over them.

Exploring novel magnetic actuators could improve the dynamics of the system. Our EM and LAPM arrays presented distinct advantages and weaknesses. The relatively slower speed and inability to change polarity in the LAPM array are bottlenecks to rapid control, and the low magnetic field strength of the EM array reduced its

ability to manipulate large numbers of particles. Therefore, it would be ideal if there were actuators that combined the high strength and density of LAPMs with the controllability of EMs.

Another direction worth exploring is developing actuation that extends interaction beyond the 2.5D regime of a horizontal plane, first to vertical and curved surfaces, and ultimately to full 3D space. The current particle and actuator design may support vertical and curved surfaces with an updated control strategy that accounts for gravity. On the other hand, realizing 3D shape configurations would likely require both a new particle design and control hardware that can independently modulate the magnetic field at different locations within a 3D volume.

6.2 Studying and Utilizing Granular Particles

Future work could further investigate how particle design, including particle geometry, material and magnetization source, influences the behavior of granular materials.

Prior work has shown that particle geometry can substantially affect particle packing and the macroscopic behavior of granular materials [27]. While we observed preliminary differences between particle geometries in our testing (Appendix C; Sec. 3.1), these observations were not the focus of this paper. A more systematic study of how particle geometry affects particle interactions and the resulting interface behaviors could provide guidance for designing particle shapes for future granular interfaces.

We also believe further exploring different particle materials could extend Granular I/O's interactivity. For example, we employed conductive PLA as the shell material to achieve a conductive cluster, which could be used in a programmable circuit design, as shown in Figure 16.

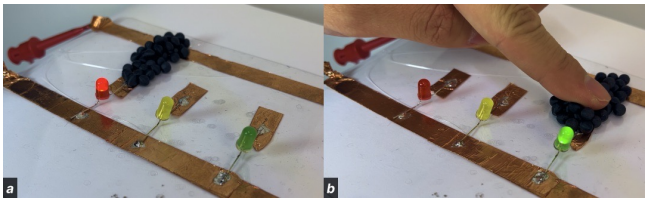


Figure 16: Programmable Circuit Application Utilizing Conductive Particles. (a) Red LED on, (b) Particles moved to turn on the green LED; the LED flickers as the user touches the particles.

Additionally, while our paper focused on an accessible particle fabrication method employing off-the-shelf magnets enclosed in 3D-printed shells, we believe other fabrication methods could be explored to miniaturize the particles below 2 mm in diameter. We could refer to prior research [25, 34] in custom fabricating magnetic material with compound materials.

6.3 Improving and Extending Malleable I/O

We would like to continue to improve the malleability of the system's sensing, actuation, and further explore additional affordances the granular materials could provide.

The current pipeline captures user input with an overhead camera and then converts it to a coarse 7 x 7 bitmap, leaving room for improvement on two fronts. On the hardware front, the external camera adds bulk and is prone to hand occlusion; embedding sensing directly into the actuation surface, similar to GaussSense [20], would make the system self-contained and occlusion-free. On the software front, the coarse bitmap captures only a fraction of the information users expressed; more advanced computer vision techniques could recover the count, positions, and 3D configurations of individual particles. Such fine-grained sensing would enable applications like 3D modeling, where users sculpt a physical cluster and the system mirrors the detected shape in a digital model.

While the current system has adequate control over the split actuation primitive, the actuation result from shape transition is still coarse compared to how a user could shape the clusters by hand. For example, the resulting shape may exhibit a hollow infill when the target shape is solid. In the future, we could explore different pixel arrangements, like hexagonal packing instead of the current square grid to improve the output shape's granularity. Moreover, alternative particle designs with more than one magnetic dipole may also improve the shape's presentation. Prior work [10] has demonstrated that modules with quadrupole magnetization can assemble into arbitrary, space-filling shapes, which could enable gapless coverage of the interaction surface and thus finer the overall presentation.

We would also like to extend the affordances of granular materials, such as drizzling, pouring, and scooping. Future systems could detect and incorporate such richer affordances for applications like fluid and dynamic system simulation.

7 Conclusion

This work proposed Granular I/O, an approach that uses an actuated magnetic field to manipulate millimeter-scale granular particles as a shape-changing display and TUI that advances programmable matter through a wide range of actuation primitives. We demonstrated the approach with two types of magnetic field control actuation hardware, magnetic particles, and software to control the system to perform actuation primitives. We evaluated their relationship with the performance of actuation primitives. A set of applications shows that Granular I/O offers the potential to provide display and interactivity for dynamic affordances. We hope that this paper will contribute to the realm of HCI and robotics to enrich programmable matter research by enabling granular, shape-changing materials.

Acknowledgments

We would like to sincerely thank the members of AxLab for their valuable feedback during the ideation and brainstorming process. We also extend our gratitude to all visitors who interacted with the prototype and provided insightful feedback that helped refine our work. We are grateful to the Electronics Development Group at the University of Chicago for providing the workspace and support needed to develop our prototypes. We also thank the University of Chicago Data Science Institute (DSI) Summer Program for supporting Clara Cui during her time at the University of Chicago. We further acknowledge the support of the Morningside Graduate Scholarship, which supported Chi Wang's studies at the University of Chicago during the course of this work.

References

[1] Anuruddha Bhattacharjee, Zhengguang Wang, Arne Schmidt, Aaron T. Becker, and Min Jun Kim. 2026. Closed-Loop Self-Assembly and Navigation of Magnetic Modular Millibots in Confined Environments. *IEEE Transactions on Automation Science and Engineering* 23 (2026), 6764–6776. https://doi.org/10.1109/TASE.2026.3675474

[2] Manuele Brambilla, Eliseo Ferrante, Mauro Birattari, and Marco Dorigo. 2013. Swarm robotics: a review from the swarm engineering perspective. *Swarm Intelligence* 7, 1 (2013), 1–41.

[3] Jialin Deng, Humphrey Yang, Aryan Saini, Urs Dominic Gaudenz, Lining Yao, Patrick Olivier, and Florian 'Floyd' Mueller. 2023. Dancing Delicacies: Designing Computational Food for Dynamic Dining Trajectories. In *Proceedings of the 2023 ACM Designing Interactive Systems Conference* (Pittsburgh, PA, USA) *(DIS '23)*. Association for Computing Machinery, New York, NY, USA, 244–262. https://doi.org/10.1145/3563657.3596021

[4] Iñigo Ezcurdia, Rafael Morales, Marco AB Andrade, and Asier Marzo. 2022. LeviPrint: Contactless Fabrication using Full Acoustic Trapping of Elongated Parts.. In *ACM SIGGRAPH 2022 conference proceedings*. 1–9.

[5] Sean Follmer, Micah Johnson, Edward Adelson, and Hiroshi Ishii. 2011. deForm: an interactive malleable surface for capturing 2.5 D arbitrary objects, tools and touch. In *Proceedings of the 24th annual ACM symposium on User interface software and technology*. 527–536.

[6] Sean Follmer, Daniel Leithinger, Alex Olwal, Nadia Cheng, and Hiroshi Ishii. 2012. Jamming User Interfaces: Programmable Particle Stiffness and Sensing for Malleable and Shape-Changing Devices. In *Proceedings of the 25th Annual ACM Symposium on User Interface Software and Technology* (Cambridge Massachusetts USA). ACM, 519–528. https://doi.org/10.1145/2380116.2380181

[7] Sean Follmer, Daniel Leithinger, Alex Olwal, Akimitsu Hogge, and Hiroshi Ishii. 2013. inFORM: Dynamic Physical Affordances and Constraints through Shape and Object Actuation. In *Proceedings of the 26th Annual ACM Symposium on User Interface Software and Technology* (St. Andrews Scotland, United Kingdom). ACM, 417–426. https://doi.org/10.1145/2501988.2502032

[8] Kyle Gilpin, Ara Knaian, and Daniela Rus. 2010. Robot pebbles: One centimeter modules for programmable matter through self-disassembly. In *2010 IEEE International Conference on Robotics and Automation*. IEEE, 2485–2492.

[9] S.C. Goldstein, J.D. Campbell, and T.C. Mowry. 2005. Programmable Matter. 38, 6 (2005), 99–101. https://doi.org/10.1109/MC.2005.198

[10] Hongri Gu, Quentin Boehler, Daniel Ahmed, and Bradley J. Nelson. 2019. Magnetic quadrupole assemblies with arbitrary shapes and magnetizations. *Science Robotics* 4, 35 (2019), eaax8977. https://doi.org/10.1126/scirobotics.aax8977 arXiv:https://www.science.org/doi/pdf/10.1126/scirobotics.aax8977

[11] Felix Heibeck, Basheer Tome, Clark Della Silva, and Hiroshi Ishii. 2015. uniMorph: Fabricating Thin Film Composites for Shape-Changing Interfaces. In *Proceedings of the 28th Annual ACM Symposium on User Interface Software & Technology* (Charlotte, NC, USA) *(UIST '15)*. Association for Computing Machinery, New York, NY, USA, 233–242. https://doi.org/10.1145/2807442.2807472

[12] Hiroshi Ishii, Dávid Lakatos, Leonardo Bonanni, and Jean-Baptiste Labrune. 2012. Radical Atoms: Beyond Tangible Bits, toward Transformable Materials. 19, 1 (2012), 38–51. https://doi.org/10.1145/2065327.2065337

[13] Hiroshi Ishii, Carlo Ratti, Ben Piper, Yao Wang, Assaf Biderman, and Eran Ben-Joseph. 2004. Bringing clay and sand into digital design—continuous tangible user interfaces. *BT technology journal* 22, 4 (2004), 287–299.

[14] Ozgun Kilic Afsar, Ali Shtarbanov, Hila Mor, Ken Nakagaki, Jack Forman, Karen Modrei, Seung Hee Jeong, Klas Hjort, Kristina Höök, and Hiroshi Ishii. 2021. OmniFiber: Integrated Fluidic Fiber Actuators for Weaving Movement based Interactions into the 'Fabric of Everyday Life'. In *The 34th Annual ACM Symposium on User Interface Software and Technology* (Virtual Event, USA) *(UIST '21)*. Association for Computing Machinery, New York, NY, USA, 1010–1026. https://doi.org/10.1145/3472749.3474802

[15] Sachiko Kodama. 2008. Dynamic ferrofluid sculpture: organic shape-changing art forms. *Commun. ACM* 51, 6 (2008), 79–81.

[16] John Lasseter. 1987. Principles of traditional animation applied to 3D computer animation. *SIGGRAPH Comput. Graph.* 21, 4 (Aug. 1987), 35–44. https://doi.org/10.1145/37402.37407

[17] Mathieu Le Goc, Lawrence H. Kim, Ali Parsaei, Jean-Daniel Fekete, Pierre Dragicevic, and Sean Follmer. 2016. Zooids: Building Blocks for Swarm User Interfaces. In *Proceedings of the 29th Annual Symposium on User Interface Software and Technology* (New York, NY, USA) *(UIST '16)*. Association for Computing Machinery, 97–109. https://doi.org/10.1145/2984511.2984547

[18] Jinha Lee, Rehmi Post, and Hiroshi Ishii. 2011. ZeroN: mid-air tangible interaction enabled by computer controlled magnetic levitation. In *Proceedings of the 24th annual ACM symposium on User interface software and technology*. 327–336.

[19] Junyang Li, Xiaojian Li, Tao Luo, Ran Wang, Chichi Liu, Shuxun Chen, Dongfang Li, Jianbo Yue, Shuk-han Cheng, and DJSR Sun. 2018. Development of a magnetic microrobot for carrying and delivering targeted cells. *Science robotics* 3, 19 (2018), eaat8829.

[20] Rong-Hao Liang, Kai-Yin Cheng, Chao-Huai Su, Chien-Ting Weng, Bing-Yu Chen, and De-Nian Yang. 2012. GaussSense: attachable stylus sensing using magnetic sensor grid. In *Proceedings of the 25th Annual ACM Symposium on User Interface Software and Technology (UIST'12), October 7 - 10, 2012, Cambridge, Ma, USA*, R. Miller (Ed.). Association for Computing Machinery, Inc., United States, 319–326. https://doi.org/10.1145/2380116.2380157 25th Annual ACM Symposium on User Interface Software and Technology (UIST 2012), UIST' 2012 ; Conference date: 07-10-2012 Through 10-10-2012.

[21] Leo Lionni. 1963. *Swimmy.* Alfred A. Knopf.

[22] Mark Marshall, Thomas Carter, Jason Alexander, and Sriram Subramanian. 2012. Ultra-tangibles: creating movable tangible objects on interactive tables. In *Proceedings of the SIGCHI Conference on Human Factors in Computing Systems*. 2185–2188.

[23] Yasushi Matoba, Toshiki Sato, Nobuhiro Takahashi, and Hideki Koike. 2012. Claytricsurface: an interactive surface with dynamic softness control capability. In *ACM SIGGRAPH 2012 Emerging Technologies*. 1–1.

[24] Y Matoba and S Sugaya. 2018. Fluidized Bed interface. In *International Display Workshops*, Vol. 2018.

[25] Alex Mazursky, Shan-Yuan Teng, Romain Nith, and Pedro Lopes. 2021. MagnetIO: Passive yet interactive soft haptic patches anywhere. In *Proceedings of the 2021 CHI Conference on Human Factors in Computing Systems*. 1–15.

[26] Wil McCarthy. 2000. Programmable Matter. 407, 6804 (2000), 569–569. https://doi.org/10.1038/35036656

[27] Kieran A. Murphy, Karin A. Dahmen, and Heinrich M. Jaeger. 2019. Transforming Mesoscale Granular Plasticity through Particle Shape. 9, 1 (2019), 011014. https://doi.org/10.1103/PhysRevX.9.011014 arXiv:1808.06271 [cond-mat]

[28] Ken Nakagaki, Sean Follmer, and Hiroshi Ishii. 2015. LineFORM: Actuated Curve Interfaces for Display, Interaction, and Constraint. In *Proceedings of the 28th Annual ACM Symposium on User Interface Software & Technology* (Charlotte, NC, USA) *(UIST '15)*. Association for Computing Machinery, New York, NY, USA, 333–339. https://doi.org/10.1145/2807442.2807452

[29] Ken Nakagaki, Pasquale Totaro, Jim Peraino, Thariq Shihipar, Chantine Akiyama, Yin Shuang, and Hiroshi Ishii. 2016. HydroMorph: Shape Changing Water Membrane for Display and Interaction. In *Proceedings of the TEI '16: Tenth International Conference on Tangible, Embedded, and Embodied Interaction* (Eindhoven, Netherlands) *(TEI '16)*. Association for Computing Machinery, New York, NY, USA, 512–517. https://doi.org/10.1145/2839462.2856517

[30] Martin Nisser, Yashaswini Makaram, Lucian Covarrubias, Amadou Yaye Bah, Faraz Faruqi, Ryo Suzuki, and Stefanie Mueller. 2022. Mixels: Fabricating Interfaces using Programmable Magnetic Pixels. In *Proceedings of the 35th Annual ACM Symposium on User Interface Software and Technology (UIST '22)*. Association for Computing Machinery, New York, NY, USA, Article 8, 12 pages. https://doi.org/10.1145/3526113.3545698

[31] Martin Nisser, Yashaswini Makaram, Faraz Faruqi, Ryo Suzuki, and Stefanie Mueller. 2022. Selective Self-Assembly using Re-Programmable Magnetic Pixels. In *2022 IEEE/RSJ International Conference on Intelligent Robots and Systems (IROS)*. IEEE, 12659–12666. https://doi.org/10.1109/IROS47612.2022.9981267

[32] Yoichi Ochiai, Takayuki Hoshi, and Jun Rekimoto. 2014. Pixie dust: graphics generated by levitated and animated objects in computational acoustic-potential field. *ACM Transactions on Graphics (TOG)* 33, 4 (2014), 1–13.

[33] Yoichi Ochiai, Takayuki Hoshi, and Jun Rekimoto. 2014. Three-dimensional mid-air acoustic manipulation by ultrasonic phased arrays. *PloS one* 9, 5 (2014), e97590.

[34] Masa Ogata and Masaaki Fukumoto. 2015. Fluxpaper: Reinventing paper with dynamic actuation powered by magnetic flux. In *Proceedings of the 33rd Annual ACM Conference on Human Factors in Computing Systems*. 29–38.

[35] Gian Pangaro, Dan Maynes-Aminzade, and Hiroshi Ishii. [n. d.]. The Actuated Workbench: Computer-Controlled Actuation in Tabletop Tangible Interfaces. ([n. d.]).

[36] Ron Pelrine, Annjoe Wong-Foy, Brian McCoy, Dennis Holeman, Rich Mahoney, Greg Myers, Jim Herson, and Tom Low. 2012. Diamagnetically Levitated Robots: An Approach to Massively Parallel Robotic Systems with Unusual Motion Properties. In *2012 IEEE International Conference on Robotics and Automation*. 739–744. https://doi.org/10.1109/ICRA.2012.6225089

[37] Laura Pruszko, Hongri Gu, Julien Bourgeois, Yann Laurillau, and Céline Coutrix. 2023. Modular tangible user interfaces: Impact of module shape and bonding strength on interaction. In *Proceedings of the Seventeenth International Conference on Tangible, Embedded, and Embodied Interaction*. 1–15.

[38] Isabel P. S. Qamar, Rainer Groh, David Holman, and Anne Roudaut. 2018. HCI meets Material Science: A Literature Review of Morphing Materials for the Design of Shape-Changing Interfaces. In *Proceedings of the 2018 CHI Conference on Human Factors in Computing Systems* (Montreal QC, Canada) *(CHI '18)*. Association for Computing Machinery, New York, NY, USA, 1–23. https://doi.org/10.1145/3173574.3173948

[39] Majken K. Rasmussen, Esben W. Pedersen, Marianne G. Petersen, and Kasper Hornbæk. 2012. Shape-changing interfaces: a review of the design space and open research questions. In *Proceedings of the SIGCHI Conference on Human Factors in Computing Systems* (Austin, Texas, USA) *(CHI '12)*. Association for

Computing Machinery, New York, NY, USA, 735–744. https://doi.org/10.1145/2207676.2207781
[40] Majken K. Rasmussen, Esben W. Pedersen, Marianne G. Petersen, and Kasper Hornbæk. 2012. Shape-Changing Interfaces: A Review of the Design Space and Open Research Questions. In *Proceedings of the SIGCHI Conference on Human Factors in Computing Systems* (New York, NY, USA) *(CHI '12)*. Association for Computing Machinery, 735–744. https://doi.org/10.1145/2207676.2207781
[41] Aditya Retnanto, Emilie Faracci, Anup Sathya, Yu-Kai Hung, and Ken Nakagaki. 2024. CARDinality: Interactive Card-shaped Robots with Locomotion and Haptics using Vibration. In *Proceedings of the 37th Annual ACM Symposium on User Interface Software and Technology* (Pittsburgh, PA, USA) *(UIST '24)*. Association for Computing Machinery, New York, NY, USA, Article 17, 14 pages. https://doi.org/10.1145/3654777.3676421
[42] John W Romanishin, Kyle Gilpin, and Daniela Rus. 2013. M-blocks: Momentum-driven, magnetic modular robots. In *2013 IEEE/RSJ International Conference on Intelligent Robots and Systems*. IEEE, 4288–4295.
[43] Anne Roudaut, Abhijit Karnik, Markus Löchtefeld, and Sriram Subramanian. 2013. Morphees: Toward High "Shape Resolution" in Self-Actuated Flexible Mobile Devices. In *Proceedings of the SIGCHI Conference on Human Factors in Computing Systems* (New York, NY, USA) *(CHI '13)*. Association for Computing Machinery, 593–602. https://doi.org/10.1145/2470654.2470738
[44] Michael Rubenstein, Christian Ahler, and Radhika Nagpal. 2012. Kilobot: A low cost scalable robot system for collective behaviors. In *2012 IEEE international conference on robotics and automation*. IEEE, 3293–3298.
[45] Deepak Ranjan Sahoo, Takuto Nakamura, Asier Marzo, Themis Omirou, Michihiro Asakawa, and Sriram Subramanian. 2016. JOLED: A Mid-air Display based on Electrostatic Rotation of Levitated Janus Objects. In *Proceedings of the 29th Annual Symposium on User Interface Software and Technology* (Tokyo, Japan) *(UIST '16)*. Association for Computing Machinery, New York, NY, USA, 437–448. https://doi.org/10.1145/2984511.2984549
[46] Deepak Ranjan Sahoo, Timothy Neate, Yutaka Tokuda, Jennifer Pearson, Simon Robinson, Sriram Subramanian, and Matt Jones. 2018. TangibleDrops: A Visio-Tactile Display Using Actuated Liquid-Metal Droplets. In *Proceedings of the 2018 CHI Conference on Human Factors in Computing Systems* (Montreal QC, Canada) *(CHI '18)*. Association for Computing Machinery, New York, NY, USA, 1–14. https://doi.org/10.1145/3173574.3173751
[47] Philipp Schoessler, Daniel Windham, Daniel Leithinger, Sean Follmer, and Hiroshi Ishii. 2015. Kinetic Blocks: Actuated Constructive Assembly for Interaction and Display. In *Proceedings of the 28th Annual ACM Symposium on User Interface Software & Technology* (New York, NY, USA) *(UIST '15)*. Association for Computing Machinery, 341–349. https://doi.org/10.1145/2807442.2807453
[48] Jungwon Seo, Jamie Paik, and Mark Yim. 2019. Modular reconfigurable robotics. *Annual Review of Control, Robotics, and Autonomous Systems* 2, 1 (2019), 63–88.
[49] Orit Shaer and Eva Hornecker. 2010. Tangible user interfaces: past, present, and future directions. *Foundations and Trends® in Human–Computer Interaction* 3, 1–2 (2010), 1–137.
[50] Lingyun Sun, Yitao Fan, Boyu Feng, Yifu Zhang, Deying Pan, Yiwen Ren, Yuyang Zhang, Qi Wang, Ye Tao, and Guanyun Wang. 2024. MagneDot: Integrated Fabrication and Actuation Methods of Dot-Based Magnetic Shape Displays. In *Proceedings of the 37th Annual ACM Symposium on User Interface Software and Technology* (Pittsburgh PA USA). ACM, 1–18. https://doi.org/10.1145/3654777.3676427
[51] Ryo Suzuki, Jun Kato, Mark D Gross, and Tom Yeh. 2018. Reactile: Programming swarm user interfaces through direct physical manipulation. In *Proceedings of the 2018 CHI Conference on Human Factors in Computing Systems*. 1–13.
[52] Ryo Suzuki, Junichi Yamaoka, Daniel Leithinger, Tom Yeh, Mark D. Gross, Yoshihiro Kawahara, and Yasuaki Kakehi. 2018. Dynablock: Dynamic 3D Printing for Instant and Reconstructable Shape Formation. In *Proceedings of the 31st Annual ACM Symposium on User Interface Software and Technology* (Berlin Germany). ACM, 99–111. https://doi.org/10.1145/3242587.3242659
[53] Tommaso Toffoli and Norman Margolus. 1991. Programmable Matter: Concepts and Realization. 47, 1 (1991), 263–272. https://doi.org/10.1016/0167-2789(91)90296-L
[54] Yutaka Tokuda, Jose Luis Berna Moya, Gianluca Memoli, Timothy Neate, Deepak Ranjan Sahoo, Simon Robinson, Jennifer Pearson, Matt Jones, and Sriram Subramanian. 2017. Programmable Liquid Matter: 2D Shape Deformation of Highly Conductive Liquid Metals in a Dynamic Electric Field. In *Proceedings of the 2017 ACM International Conference on Interactive Surfaces and Spaces* (Brighton, United Kingdom) *(ISS'17)*. Association for Computing Machinery, New York, NY, USA, 142–150. https://doi.org/10.1145/3132272.3134132
[55] Udayan Umapathi, Samantha Chin, Patrick Shin, Dimitris Koutentakis, and Hiroshi Ishii. 2018. Scaling Electrowetting with Printed Circuit Boards for Large Area Droplet Manipulation. 3, 26 (2018), 1475–1483. https://doi.org/10.1557/adv.2018.331
[56] Udayan Umapathi, Patrick Shin, Ken Nakagaki, Daniel Leithinger, and Hiroshi Ishii. 2018. Programmable droplets for interaction. In *Extended Abstracts of the 2018 CHI Conference on Human Factors in Computing Systems*. 1–1.
[57] Akira Wakita, Akito Nakano, and Nobuhiro Kobayashi. 2010. Programmable blobs: a rheologic interface for organic shape design. In *Proceedings of the fifth international conference on Tangible, embedded, and embodied interaction*. 273–276.
[58] Malte Weiss, Florian Schwarz, Simon Jakubowski, and Jan Borchers. 2010. Madgets: Actuating Widgets on Interactive Tabletops. In *Proceedings of the 23nd Annual ACM Symposium on User Interface Software and Technology* (New York New York USA). ACM, 293–302. https://doi.org/10.1145/1866029.1866075
[59] Mikael Wiberg. 2018. *The Materiality of Interaction: Notes on the Materials of Interaction Design*. The MIT Press. https://doi.org/10.7551/mitpress/10427.001.0001
[60] Wikipedia contributors. 2025. Inbetweening — Wikipedia, The Free Encyclopedia. https://en.wikipedia.org/w/index.php?title=Inbetweening&oldid=1329062308. [Online; accessed 24-July-2026].
[61] Junichi Yamaoka. 2020. Rapid and Shape-Changing Digital Fabrication Using Magnetic Thermoplastic Material. In *ACM SIGGRAPH 2020 Posters*. ACM, 1–2.
[62] Kijun Yang, Sukyoung Won, Jeong Eun Park, Jisoo Jeon, and Jeong Jae Wie. 2025. Magnetic Swarm Intelligence of Mass-Produced, Programmable Microrobot Assemblies for Versatile Task Execution. 3, 4 (2025). https://doi.org/10.1016/j.device.2024.100626
[63] Kentaro Yasu. 2022. MagneShape: A Non-electrical Pin-Based Shape-Changing Display. In *Proceedings of the 35th Annual ACM Symposium on User Interface Software and Technology (UIST '22)*. Association for Computing Machinery, New York, NY, USA, Article 71, 12 pages. https://doi.org/10.1145/3526113.3545645
[64] Kentaro Yasu. 2024. MagneSwift: Low-Cost, Interactive Shape Display Leveraging Magnetic Materials. In *Proceedings of the 2024 CHI Conference on Human Factors in Computing Systems (CHI '24)*. Association for Computing Machinery, New York, NY, USA, Article 863, 11 pages. https://doi.org/10.1145/3613904.3642058
[65] Mark Yim, Ying Zhang, and David Duff. 2002. Modular robots. *IEEE Spectrum* 39, 2 (2002), 30–34.

A Tweening Frame Generation Algorithm

The Tweening Frame Algorithm is described in the following pseudocode in Algorithm 1. Sample output frames are shown in Figure 17.

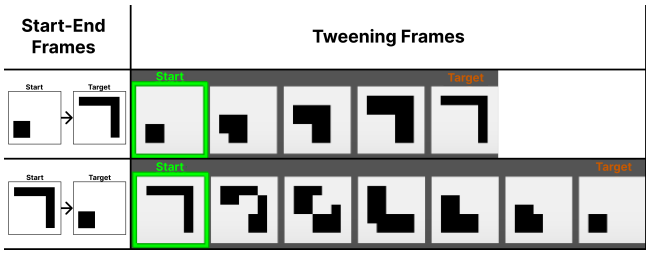


Figure 17: Tweening frames generated by the software as they appear in the GUI. (The frame count difference comes from the result by following the algorithm.)

B Magnetic Field Measurement

In this section, we will share the magnetic filed strength measurement from the the permanent magnet used in the LAPM device. Figure 18 shows the measurement setup. The origin O is at the center of top surface of the cylinder magnet. Axial measurement point P_1 is on the center axis at height h. Radio measurement point P_2 is on the same horizontal surface of the magnet's top surface, with distance r to the center.

B_1 measures the vertical component of the magnetic field at P_1, B_2 and B_3 measures the vertical and radio component of the magnetic field at P_2.

The B_1, B_2 and B_3 measurement results are shown in the Figure19, 20, 21. All the y axis are log-scaled and the x axis are linear scaled.

Algorithm 1 Tweening Frame Generation

Require: Start pattern S, Target pattern T, Max steps K
Ensure: Sequence of tweening frames F

CurrentFrame ← S
Add CurrentFrame to F
for $step$ = 1 to K **do**
  Find all pixel **Candidates** where:
    1. Pixel is adjacent to CurrentFrame
    2. Pixel is currently OFF
    3. Pixel's closest target is also OFF
  if no Candidates found **then**
    break
  end if
  d_min ← minimum distance from any Candidate to T
  Grow: Add all pixels in Candidates with distance d_min to CurrentFrame
  d_max ← maximum distance from any Pixel in CurrentFrame to T
  if $d_max > 0$ **then**
    Trim-off Tails: Remove all pixels with distance d_max from CurrentFrame
  end if
  Add CurrentFrame to F
  if CurrentFrame matches T **then**
    break
  end if
end for
return F

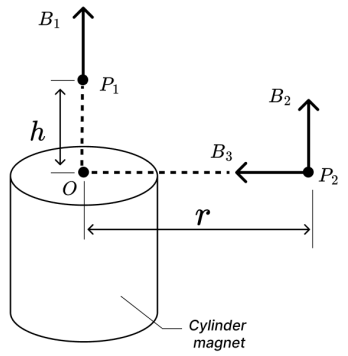


Figure 18: Measurement Setup Diagram

Discussion From the measurements, we can see that the magnetic field strength generally forms into a straight line, indicating that at the measuring range, the magnetic field strength decays at an approximately exponential rate.

We can also see that, when $r = 15mm$, B_3 roughly drop to 7 mT. This indicates that the magnetic field strength drops to around background level after reaching the center of the next pixel. This means that the magnet's effective range is limited to its neighboring pixels.

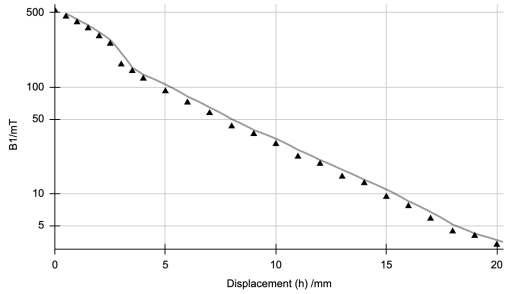


Figure 19: Axial magnetic field B_1 vs. vertical displacement h

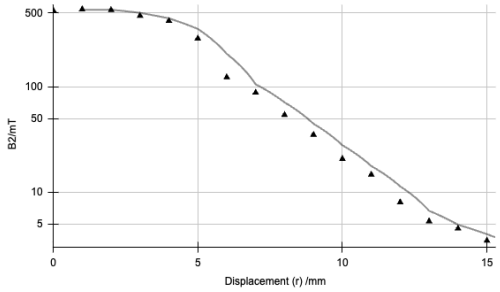


Figure 20: Vertical components B_2 vs. radial displacement r

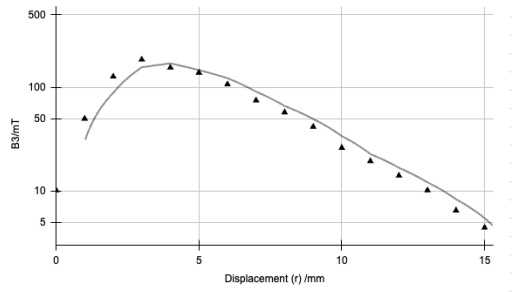


Figure 21: Radial components B_3 vs. radial displacement r

C Particle Designs and Actuation

In this section, we show how the different particle designs, including particle size, shape, as well as cluster size, affects the performance of the proposed **move** and **split** actuation primitives for both EM and LAPM arrays. Specifically, we evaluated the relationship between *Particle Size (= 4, 5, 7 mm)*, *Geometry(= Sphere, Cube)*, *Number of Particles in Cluster* and the success rate of two Actuation Primitives: the default *Move* and *Split*.

To decide on different numbers of particles in each cluster, we built a ratio between the scale of the control magnet pixel spacing and the scale per cluster, ensuring consistency. Let l_{pixel} be the spacing of the control magnet pixels, l_{particle} be the particle size, and n be the number of particles, then we can define the cluster size index as $k = \frac{n \cdot l_{\text{particle}}}{l_{\text{pixel}}}$. We carried out the evaluation based on

two commonly used values: $k = 2$ for small clusters and $k = 5$ for large clusters.

Study Procedure:

(1) Prepare the cluster of particles with the specific Particle Size, Geometry and Particle Number.
(2) Run the **move**, **split** Actuation Primitives
(3) For each cluster, repeat step 2 10 times on each control hardware.

Cluster Properties				AP Success Number (out of 10 Trials)			
Particle Size, Geometry, and Cluster Size	Particle Number*		Embedded Magnets	Move**		Split	
	LAPM	EM		LAPM	EM	LAPM	EM
4mm ○ - small cluster (k=2)	8	13	3mm ○	10	3	9	2
4mm ○ - large cluster (k=5)	19	32	3mm ○	10	4	10	4
5mm ○ - small cluster (k=2)	6	10	3mm ○	10	5	10	10
5mm ○ - large cluster (k=5)	15	25	3mm ○	9	8	10	10
7mm ○ - small cluster (k=2)	5	8	3mm ○	10	0	7	10
7mm ○ - large cluster (k=5)	10	18	3mm ○	10	8	7	10
5mm □ - small cluster (k=2)	6	10	3mm ○	7	0	6	10
5mm □ - large cluster (k=5)	15	25	3mm ○	1	0	10	10
3mm ○ - small cluster (k=2)	10	17	1.5mm □	10	1	10	4
3mm ○ - large cluster (k=5)	25	42	1.5mm □	10	4	10	3
3mm □ - small cluster (k=2)	10	17	1.5mm □	10	2	10	10
3mm □ - large cluster (k=5)	25	42	1.5mm □	4	3	10	10
			Overall Success Rate:	87%	33%	89%	73%

Figure 22: Actuation Primitive evaluation across varying particle designs and cluster scales

Results: The results are as shown in Figure 22. From the results, we can see that in general, the 5 mm sphere particle with 3 mm sphere magnet insert works the best across cluster size, AP and control hardware. Thus, we mainly use this particle design for developing applications. Most particle designs performs well for **split**, and **move** with EM are the most demanding AP that works well with only large cluster size of 5 mm sphere particles with 3 mm magnet insert. We recommend users should not worry too much about fine tuning the particle design when using LAPM systems, but should be mindful about choosing the particle design when working with EM system.

D System Setup

Figure 23 shows the arrangement of the actuator prototype, with an overhead camera mounted ~20 cm above the interaction surface.



Figure 23: System Setup